

Thermomechanical Studies of Poly(aniline)/Poly(methyl methacrylate) Blends: Relationship with Conducting Properties

Jérôme Fraysse,^{†,§} Jérôme Planès,^{*,†} Alain Dufresne,[‡] and Ali Guermache[†]

Laboratoire de Physique des Métaux Synthétiques, UMR 5819 CEA-CNRS-UJF, CEA-Grenoble/DRFMC/SI3M, 17, rue des Martyrs, F-38054 Grenoble, Cedex 9, France, and Centre de Recherches sur les Macromolécules Végétales (CERMAV-CNRS), Université Joseph Fourier, B. P. 53, F-38041 Grenoble, Cedex 9, France

Received March 12, 2001; Revised Manuscript Received August 10, 2001

ABSTRACT: We report on the first dynamic mechanical studies of blends of conducting polymer poly(aniline) (PANI) in an insulating matrix that exhibit ultralow electrical percolation threshold. Whereas the matrix undergoes an irreversible flow slightly above its glass–rubber transition temperature, blends with PANI mass fraction as low as 1% show a well-defined rubber plateau with a stability range of ca. 100 K. These results corroborate the image of a ramified network of conducting phase, inferred from electrical results. In situ resistance measurements during tensile testing also probe the conductive network. The increase of conductivity in the elastic regime could be interpreted as a consequence of a better alignment of PANI bundles.

1. Introduction

The interest in blends of the conducting polymer PANI with traditional insulating matrices is mainly due to the extremely low electrical percolation threshold that can be reached via cosolution processing. It is known since 1993¹ that a macroscopic conductivity is still observable for weight fractions of camphor sulfonic acid (CSA) doped PANI in PMMA less than 1%. It is argued that, due to such a low threshold (down to 0.07%²), the main properties of the matrix are retained, e.g., optical transparency and mechanical behavior. However, no mechanical testing has been performed on those samples to give a quantitative assessment.

Such experiments not only are useful for mechanical characterizations but also give a closer insight into the microstructure of the blend. Electrical percolation is assumed to occur on a ramified network of PANI bundles, but it is known that the hopping mechanism (and thus charge carrier tunneling) plays a major role in the transport properties of these systems. The very small scale dispersion of PANI has been checked by real space imaging techniques (transmission electron microscopy,^{1,3} atomic force microscopy³). But nothing is known about the nature of the connectivity and the strength of contacts between bundles. In that sense, DMA and tensile testing are good means of probing the nature of the network, as has been done with other types of polymer fillers, either insulating like cellulose whiskers in PVC,⁴ cellulose whiskers in starch,⁵ and starch in thermoplastics⁶ or conducting like carbon black in elastomer.⁷

In this paper, we present the first thermomechanical studies of PANI(CSA)/PMMA, showing that a mechanical percolation indeed occurs in the conductive phase. Section 2 explains the sample preparation and recalls

the experimental methods. Section 3 gives the results of DMA experiments for three series of samples with various plasticizer contents. Section 4 presents the analysis through Takayanagi's model modified by percolation. Preliminary tensile tests coupled with resistance measurements on a similar system are discussed in section 5. Conclusions are given in section 6.

2. Experimental Section

Samples were fabricated in the following way, thoroughly described in ref 8. Poly(aniline) in the oxidation state of emeraldine base (PANI EB) and the protoning agent CSA were transferred to *m*-cresol (MC). The suspension was stirred for 1 week and centrifuged. Only the nonsedimented fraction was used. The concentration of PANI in solution was determined by measuring the difference between the initial EB mass taken for protonation and the mass of sedimented PANI after its deprotonation. PANI EB used had an inherent viscosity of 1.49 dL/g at 25 °C (0.1 wt % of EB in H₂SO₄).

Solutions of PMMA in *m*-cresol were prepared with three different mass ratios x of plasticizer dibutyl phthalate (DBPh): $x = \text{DBPh}/\text{PMMA} = 0, 0.25, \text{ or } 0.35$. Number molecular average weight of PMMA is $M_n = 45\,800$, and polydispersity $M_w/M_n = 1.9$.

PANI/PMMA blends were prepared by mixing nonplasticized and plasticized solutions of PMMA with appropriate amounts of solutions of CSA-protonated PANI to obtain three series with PANI contents p between ca. 0.05 and 5 wt %. p denotes the ratio percent of PANI EB mass to (PANI EB + CSA + PMMA + DBPh) mass. Ultimately, free-standing films were cast by evaporation of *m*-cresol at 40 °C from all these homogeneous solutions. A typical thickness of the samples was between 25 and 100 μm .

The same process was used for PANI doped by di(2-ethylhexyl) ester of phthalosulfonic acid (DEHEPSA) in dichloroacetic acid (DCAA) as solvent.⁹ Blends of PANI(DEHEPSA) with plasticized PMMA ($x = 0.35$) were also prepared in the same manner from DCAA cosolutions.

Thermomechanical investigations were done using a Rheometrics RSA II spectrometer in the tensile mode. Dynamic mechanical tests were carried out in a temperature (T) range of 250–550 K, around the glass–rubber temperature transition of the matrix ($T_g \approx 330\text{ K}$). The tests were performed in the linear viscoelasticity region (maximum strain $\epsilon \leq 5 \times 10^{-4}$), using isochronal mode at 1 Hz with 3 K temperature incre-

[†] Laboratoire de Physique des Métaux Synthétiques.

[‡] Université Joseph Fourier.

[§] Present address: von Klitzing Group, Max-Planck-Institut für Festkörperforschung, Heisenbergstrasse 1, D-70569 Stuttgart, Germany.

* Corresponding author: e-mail jplanes@cea.fr.

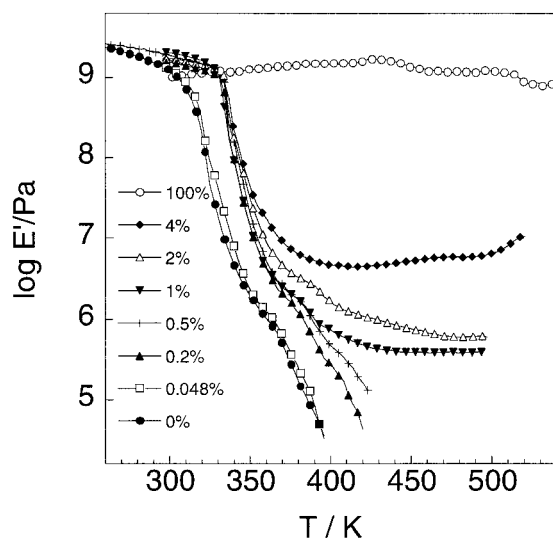


Figure 1. Thermal dependence of the storage modulus (logarithmic scale) for PANI(CSA)/PMMA($x = 0$) blends with PANI content between 0 and 100%.

ments. The samples were cut as thin rectangular strips with typical dimensions of $20 \times 6 \times 0.1 \text{ mm}^3$. The setup measures the complex tensile modulus E^* , i.e., the storage component E' and the loss component E'' . In the present work, results are displayed through E' and the loss angle tangent: $\tan \delta = E''/E'$.

An Instron tensiometer with a 10 N load cell was used to perform in situ resistance measurement during uniaxial stretching on rectangular samples with typical dimensions $12 \times 5 \times 0.1 \text{ mm}^3$. Gold pads were evaporated at both ends of the samples, contacted to thin gold wires via metallic tape, and electrically isolated from and clamped by the jaws of the tensile machine. The resistivity measured by this two-probe method was identical to the classical four-probe resistivity. All measurements were performed at room temperature (RT), below T_g . The strain rate was $\dot{\epsilon} = 0.7 \times 10^{-3} \text{ s}^{-1}$ (0.5 mm/min). Because of the geometric deformation, the resistance value is given instead of the resistivity.

3. Dynamic Mechanical Analysis

Figure 1 displays the logarithm of the storage tensile modulus E' vs T measured on the nonplasticized samples. The curve obtained from pure PMMA film (filled circles) cast from MC solution is characteristic of thermoplastics with, however, a hardly visible rubbery state, due to the low PMMA molecular weight. Above 300 K, E' rapidly decreases with temperature, indicating the transition of PMMA from the glassy state toward the rubbery state (transition temperature $T_g \approx 330 \text{ K}$). In the terminal zone, the relaxed elastic modulus slumps due to irreversible flow, and the setup fails to measure it.

The open circle symbols correspond to PANI film cast from MC solution. Thermomechanical features of this film (and especially T_g) are not fully ascertained yet. However, our data clearly show that elastic modulus remains high ($\sim 1 \text{ GPa}$) over the whole investigated temperature range. That is not surprising since such films are known to be semicrystalline.¹⁰ The crystallinity degree is approximately 25%, and the size of the crystallites, acting as reticulation centers, reaches 5–10 nm.¹⁰ The curves obtained for the blends could be divided into two groups. First, the addition of PANI essentially does not induce any significant change in the shape of the curves. This behavior holds for concentrations up to 0.5 wt % PANI. For more concentrated blends, we notice a dramatic change in the shape of the

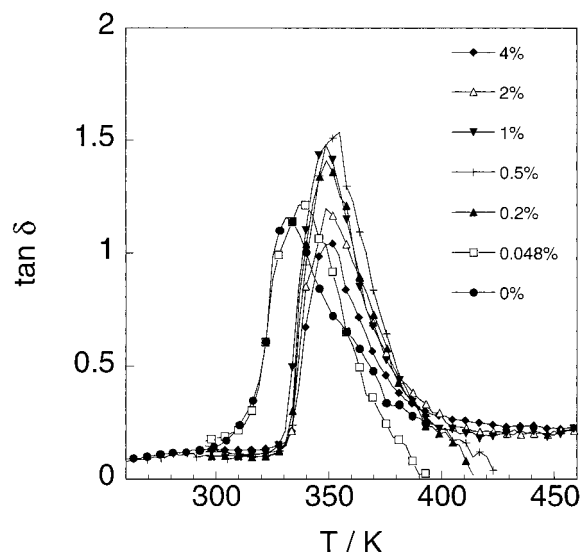


Figure 2. Thermal dependence of the loss angle tangent for PANI(CSA)/PMMA($x = 0$) blends with PANI content between 0 and 4%.

curves: the relaxed elastic modulus keeps a constant value over a large temperature range (from 400 to 500 K) until the sample breaks, because of irreversible chemical degradation. This transition occurs for PANI content between 0.5 and 1%. Moreover, the value of the relaxed modulus is p -dependent and increases by 1 order of magnitude (from $\log E' = 5.6$ to $\log E' = 6.6$) as p increases from 1 to 4 wt %. Furthermore, we notice an increase of the modulus above 500 K for $p = 4\%$. Pure PANI exhibits a similar increase in E' at identical temperature,¹¹ which is attributed to the reticulation of the chains. We suppose that the same mechanism occurs here.

Figure 2 shows the loss angle tangent $\tan \delta$ vs T for blends with PANI contents in the range 0–4 wt %. For the experimental conditions we used, the maximum in $\tan \delta$ is generally associated with T_g . The curve corresponding to pure PMMA presents a main loss angle peak at 330 K. The jump of T_g values for the major part of blend samples is at least partly due to the temperature controller and is not recovered for other x values (Figure 3). We however notice, as expected for PMMA relaxing entities, that the integrated area under the curve decreases with addition of PANI. That is especially clear when comparing $p = 1, 2$, and 4%.

Adding plasticizer leaves preceding results qualitatively unchanged. Slight quantitative discrepancies have to be mentioned. First, as expected for a plasticizing effect, a small but global decrease of T_g is observed. Whereas T_g lies in the range 330–350 K for $x = 0$ and $0 \leq p \leq 4\%$, T_g lies in the range 320–335 and 320–330 K for respectively $x = 0.25$, $0 \leq p \leq 4\%$ and $x = 0.35$, $0 \leq p \leq 1\%$. Plots of E' vs T for $x = 0.25$ and $x = 0.35$ series show a transition between two very distinct mechanical behaviors for $T > T_g$, similarly to the $x = 0$ case. Transition takes place for $0.5 < p < 1\%$ with $x = 0.25$ (not shown) and for a lower value $0.3 < p < 0.5\%$ with $x = 0.35$ (Figure 3). We are thus tempted to define experimentally a PANI content threshold p_m , which characterizes the transition. Below p_m an irreversible flow rapidly occurs for $T > T_g$, and above p_m a relaxed modulus can be measured and remains constant over a large temperature range.

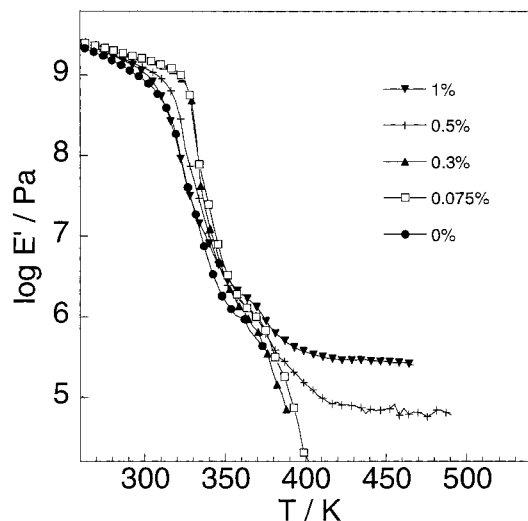


Figure 3. Thermal dependence of the storage modulus (logarithmic scale) for PANI(CSA)/PMMA($x = 0.35$) blends with PANI content between 0 and 1%.

4. Mechanical Coupling Model

To make a quantitative modeling of the observed behavior, we have to explicitly introduce the percolation concept. As a matter of fact, due to the very small fraction of PANI, any mixing law based on effective medium is reduced to its linear development at $p \rightarrow 0$ and cannot account for our results.

As already proposed by Ouali et al.,¹² we start from Takayanagi's model¹³ which combines series and parallel components. The system consists of a rigid (R) and a soft (S) phase of respective mass fraction¹⁴ p and $1 - p$. We suppose that the rigid phase percolates, and we denote by ψ the mass fraction occupied by the rigid phase belonging to the infinite cluster. Indeed ψ represents the part that really reinforces the material. The complementary fraction $(1 - \psi)$ is thus composed of the soft phase in a proportion λ and of the remaining rigid phase in finite clusters in proportion $(1 - \lambda)$. Therefore, the mechanical behavior of such a system would be described as schematically shown in Figure 4. The Young modulus of the system depicted in Figure 4 is written as

$$E^* = E_R^* + [\lambda/E_S^* + (1 - \lambda)/E_R^*]^{-1}$$

Parameters λ , ψ , and p are related by

$$p = \psi + (1 - \lambda)(1 - \psi)$$

Takayanagi's formula thus reads

$$\frac{E^*}{E_R^*} = \frac{(1 - 2\psi + \psi p)E_S^* + \psi(1 - p)E_R^*}{(p - \psi)E_S^* + (1 - p)E_R^*} \quad (1)$$

The additional percolation hypothesis implies

$$\psi = 0 \quad \text{for } p < p_m$$

and

$$\psi = \psi_0 (p - p_m)^b \quad \text{for } p > p_m \quad (2)$$

p_m is the critical mass fraction of rigid phase at the percolation threshold, and b is the corresponding critical exponent.

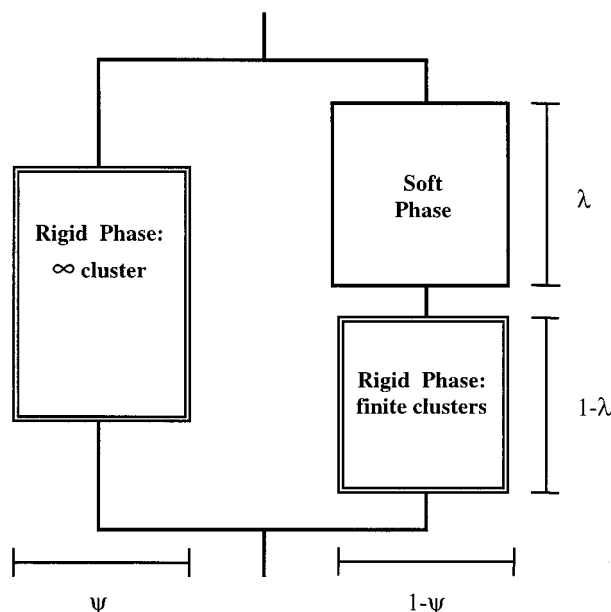


Figure 4. Schematic representation of the series-parallel model of Takayanagi. In Ouali's extension, ψ depends on concentration p according to the percolation scaling law.

Application of this model to our data needs the knowledge of pure components $E_R^*(T)$ and $E_S^*(T)$. The ill-shaped PANI data (Figure 1) obviously influence the values computed by eq 1. The limited sensitivity of DMA force sensor impedes the determination of $E_S^*(T)$ for $T > 400$ K. If we set $E_S^* = 0$, we see that $E^* = \psi E_R^*$. This can be used to estimate parameters p_m and b in eq 2 from $E^*(p)$ at e.g. $T = 450$ K. We find $p_m = 0.6\%$ and $b = 0.93$. Accuracy is strongly limited by the small number of samples with $p > p_m$. Nevertheless, use of this set of parameters yields the fitted curves displayed in Figure 5 as E' and $\tan \delta$. It is well suited to reproduce the main features of $E^*(p, T)$ above p_m , namely the existence of the rubber plateau, the increase of E' , and the decrease of maximum of $\tan \delta$ with increasing p .

Let us note that the temperature shift between data and model only reflects the shift seen in Figure 1 between PMMA and high p blends curves (section 3). For this reason, we do not discuss possible variations of T_g with p in this study. We shall anyway recall that the model used does not take into account any interaction between matrix and filler and therefore is not able to explain the T_g shift, if any. It is seen, in the model curves of Figure 5, that, as p decreases, $\max(\tan \delta)$ occurs at increasing T and peak broadens toward high T . This is correlated to the increase of the storage modulus drop during the glass-rubber transition. Experimental data seem not to follow this trend. If this effect is confirmed in future experiments, this could be assigned to interaction effects.

We shall also mention that the whole data set analyzed here corresponds to experiments in room atmosphere. PANI is known to be sensitive to O_2 , which is the most efficient agent of aging.¹⁵ Blending PANI with PMMA at small fractions partly acts as an encapsulation and protects PANI from degradation. This effect is a possible source of nonidentical behavior between pure PANI and blends; the higher T , the more pronounced. A DMA scan of PANI in a nitrogen atmosphere indeed starts to deviate from the one shown in Figure 1 at $T > 450$ K: the storage modulus decreases. Renewing all the experiments with the blends in a

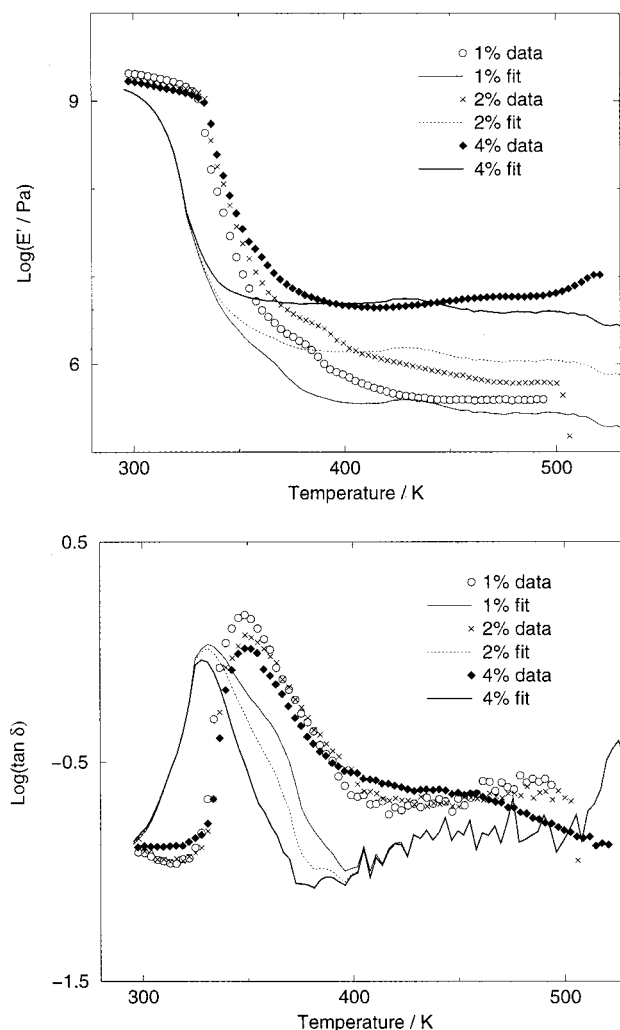


Figure 5. Modelization of the storage modulus E' and the loss angle tangent $\tan \delta$ according to eq 1 modified by percolation (eq 2), for blends with concentration p above 1%.

nitrogen atmosphere would provide us with a better estimation of this effect.

5. Tensile Testing

Experiments have been performed with PANI(DEHEPSA) cast from DCAA because PANI(CSA) cast from *m*-cresol shows poor mechanical properties. DEHEPSA dopant has been specially designed to improve plastic behavior of PANI,⁹ and preliminary results show that elongation at break increases from a few percent (with CSA) to 40% at least (with DEHEPSA).¹⁶ Electronic transport properties of both systems are extremely close to each other⁹ and so are their blends with PMMA. In particular, a very low electrical percolation threshold is found,⁹ and the peculiar temperature dependence of percolation parameters observed in PANI(CSA)/PMMA² is retrieved here.¹⁷

Strain–stress curves for pure PANI ($p = 100$) and 1% blend ($p = 1$) are shown in Figure 6 in nominal values, $\sigma_{\text{nom}} = F/S_0$, $\epsilon_{\text{nom}} = \Delta L/L_0$, with F the force, S_0 ($\approx 0.5 \text{ mm}^2$ typically) the initial section, ΔL the elongation, and L_0 ($\approx 12 \text{ mm}$ typically) the initial length between clamps. Curves are characteristic of ductile behavior with uniform extension ($p = 100$) or cold-drawing with yield point $\sigma_y = 15 \text{ MPa}$, $\epsilon_y = 0.1$ ($p = 1$). Room temperature, which was ca. $300 \pm 2 \text{ K}$, is not far from $T_g \approx 320 \text{ K}$ for plasticized PMMA in the blend, and the tangent modu-

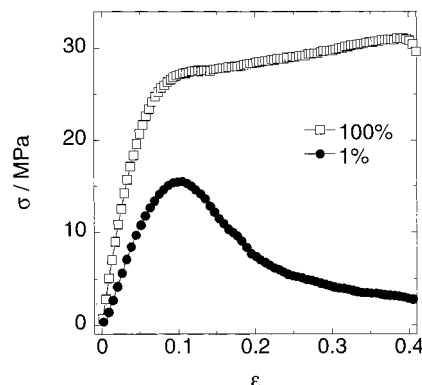


Figure 6. Stress–strain curves of PANI(DEHEPSA) and PANI(DEHEPSA)/PMMA($x = 0.35$) blend with $p = 1\%$, measured in tensile mode.

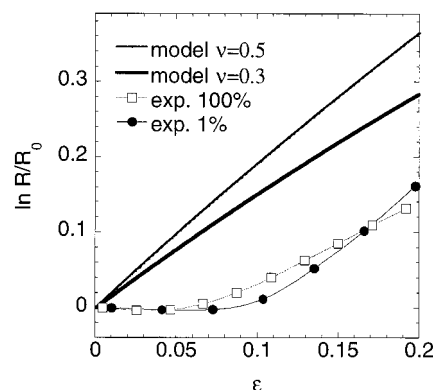


Figure 7. Relative resistance of PANI(DEHEPSA) and PANI(DEHEPSA)/PMMA($x = 0.35$) blend with $p = 1\%$ as a function of strain during tensile testing. Continuous curves are theoretical behaviors assuming a material of constant resistivity and Poisson ratio ν equal to 0.5 or 0.3.

lus at 300 K is already lower (by a factor of 3–5) than its glassy value.

The relative variation of resistance (R_0 is the initial resistance) for both samples is displayed in Figure 7. Curves are very similar and present two parts. R/R_0 is almost constant (with a slight minimum) up to $\epsilon = 0.07$ ($p = 100$) or 0.09 ($p = 1$) and then increases with ϵ . We can compare the measurements to the expected values corresponding to the geometrical deformation at constant resistivity. Those values depend on the deformation mechanism which is not precisely known but whose effect can be bounded by use of various Poisson ratio ν . Let

$$\nu = \frac{1}{2} \left(1 - \frac{1}{V} \frac{dV}{d\epsilon} \right)$$

Thus

$$\ln \frac{V}{V_0} = (1 - 2\nu)\epsilon$$

and

$$\ln \frac{R}{R_0} = \ln \frac{L^2}{L_0^2} \frac{V_0}{V} = 2 \ln(1 + \epsilon) - (1 - 2\nu)\epsilon$$

Curves for $\nu = 0.5$ (the rubber limit) and $\nu = 0.3$ (mimicking vitreous behavior) are superimposed in Figure 7. One can see, first, that the constant resistivity assumption is far from being fulfilled at low strain and,

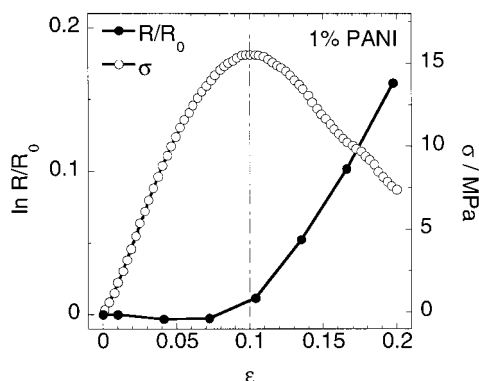


Figure 8. Correlation between stress and resistance during tensile testing for PANI(DEHEPSA)/PMMA($x = 0.35$) blend with $p = 1\%$.

second, that the increase at high strain is rather well accounted for by this hypothesis. The maximum increase in conductivity is, depending on ν , 10–15% for $p = 100$ and 15–20% for $p = 1$.

Plotting R/R_0 and σ simultaneously as in Figure 8 emphasizes the correlation between plastic and electrical behaviors. In the elastic regime, the deformation of the PANI network results in an increase of conductivity (in the strain direction). This is a traditional method of improving conductive properties of conducting polymers by aligning fibers or bundles, thus reducing disorder,¹⁸ and the same process is likely to occur here, even if the temperature is not optimized for such a goal. In the plastic regime, this effect is either suppressed or compensated by irreversible alteration of the network. The similarities between $p = 100$ and $p = 1$ and the absence of depercolation (catastrophic increase of R) before break occurs (even at lower p) are indicators of the strength of PANI network inside the blends.

6. Discussion

Mechanical properties of doped conducting polymers have long been a meaningless question because of insolubility and infusibility. Since the discovery of the solubility of PANI(CSA) in *m*-cresol, its thermomechanical behavior is still controversial. It has generally been argued¹⁹ that no glass–rubber transition occurs before thermal degradation of CSA dopant (ca. 500 K) and PANI itself. Conversely, Durham's group shows a DMA scan where the α transition, located at 445 K, is coherent with $T_g = 425$ K determined by differential scanning calorimetry.²⁰ Peaks at lower T are attributed to water and residual solvent loss, modifying H-bonding in the system. In the case of undoped PANI (EB form, with the same solvent), properties are not better established.¹⁹ By DMA, Lesueur et al.¹¹ suggest that $T_g = 475$ K. DMA scans of PANI(DEHEPSA) cast from DCAA (or even other solvents) look more similar to traditional thermoplastics (see Figures 5 and 6 in ref 9). Nevertheless, attribution of relaxation mechanisms is not doubtless. There is a strong similarity between Figures 5 and 6 in ref 9 and Figure 3 in ref 20, and it is likely that $T_g = 450$ K.

The poor knowledge of thermomechanical properties of the “filler” obviously complicates the analysis of blend properties. The latter are influenced by the nature of polymer–polymer interactions. Segregation as probed by electrical percolation behavior at ultralow threshold and morphological studies (TEM, AFM) is indicative of a low level of interaction. But this should be probed

more accurately by DSC, evidencing a continuous change in T_g with p or not. In the case of PANI(CSA)/nylon 6 blends, such experiments were carried out and concluded, in accordance with small-angle neutron scattering, that interactions are very limited.¹⁹

To our knowledge, there are no other example of “mechanical percolation” at such low threshold. We refer to percolation with prudence because the first series of experiments has to be improved and raises several questions, especially in comparison to conductive properties. First, we are facing the problem of the force sensor sensitivity which, at a given T , abruptly separates “rubbery” from “creeped” samples, according to E' being greater or lower than ca. 0.5 MPa. This reinforces the threshold effect. A reducing force mode, to adjust the static force during sample relaxation, should be used in the future. To this respect, conductivity measurements benefit from a much wider dynamic range. The present conclusion is that the mechanical threshold (0.5–1%) is significantly higher than the electrical one (0.04–0.07%). Assessing this effect will be of great interest for its implication in the conduction mechanisms. Because the percolation scaling law perfectly describes the p dependence of conductivity without any deviation in the 0.5–1% range (or even below), it would mean that the hopping mechanism (or, say, how it is reflected in a macroscopic measurement) is not influenced by the presence or absence of mechanical connectivity of the network.

One shall also take into account another difference in experimental conditions. Whereas conductivity is measured between 4 and 300 K, in which range the electrical threshold p_c does not vary, the percolation behavior of the storage modulus is observed between 400 and 500 K. No meaningful information can be extracted at RT or below because the mechanical contrast between PANI, and PMMA is too small in the glassy state. The thermal stability of the network thus deserves attention and need to be questioned. A partial response is given by Yang et al.,²¹ who have studied the problem in exactly the same system, but only for concentration above 1%. Their conclusions, derived from TEM observations, are that the network structure starts to degrade only at 500 K. Nevertheless, at 450 K, part of CSA have migrated to form crystallites, and consequently the conductivity is significantly lowered. It is known that CSA molecules play a major role in the partially crystalline structure of doped PANI,¹⁰ itself intimately linked to conductive properties. Whether they play such a role in viscoelastic properties is not known. The flat appearance of $E'(T)$ in the 400–500 K could signify that it is not the case. Concomitantly, this would also make us think that the mechanical threshold p_m does not depend on T too much. Very careful experiments are needed to prove this point.

Comparisons of electrical and mechanical behaviors in conducting blends are seldom in the literature. Among similar systems are carbon black (CB)/polymer composites, thoroughly studied and used. A major difference takes place between those composites and our blends, due to the stronger contrast of materials nature. As a matter of fact, temperature and deformation act differently on CB composites and principally lead to percolation/depercolation transitions. In a tensile test, for instance, the resistivity shows a sharp increase as soon as the strain starts,⁷ which is attributed to the breakage of the CB network. Among PANI blends

experiments we are aware of, let us quote the work by Ho et al.²² concerning PANI(DBSA)/PU where the dopant DBSA is *n*-dodecylbenzenesulfonic acid and PU is polyurethane with a chain extender. It is claimed that in this system tensile strength exhibits a sharp increase as PANI content is raised, as well as conductivity, but at higher content (typically 20% instead of 10%). This reminds our observation of a shift between mechanical and electrical thresholds in PANI(CSA)/PMMA and also in PANI(DEHEPSA)/PMMA when considering yield stress (not shown here).

As a conclusion, measurements of the thermomechanical behavior of PANI(CSA)/PMMA blends, which exhibit ultralow electrical percolation threshold, have shown that the onset of "mechanical percolation" does occur at some low content of PANI, typically 1%. This is evidenced by the presence of a well-defined rubber plateau with E' in the MPa range for T in the 400–500 K range, whereas this plateau vanishes for pure matrix or lower PANI contents. This effect, which was not reported until now, needs more accurate experiments to be well characterized: whether the electrical and mechanical thresholds differ or not is especially interesting for the detailed analysis of structure–properties relationship in this disordered conducting systems. The conductivity enhancement observed in the resistance–tensile test coupled experiments corroborates the image of a rather strong network and the influence of the local arrangement of conductive bundles on the macroscopic transport properties.

References and Notes

- (1) Yang, C. Y.; Cao, Y.; Smith, P.; Heeger, A. J. *Synth. Met.* **1993**, *53*, 293–301.
- (2) Fraysse, J.; Planès, J. *Phys. Status Solidi B* **2000**, *218*, 273–277.
- (3) Planès, J.; Samson, Y.; Cheguettine, Y. *Appl. Phys. Lett.* **1999**, *75*, 1395–1397.
- (4) Chazeau, L.; Paillet, M.; Cavaillé, J. Y. *J. Polym. Sci., Part B: Polym. Phys.* **1999**, *37*, 2151–2164.
- (5) Chazeau, L.; Cavaillé, J. Y.; Canova, G.; Dendievel, R.; Bouthierin, B. *J. Appl. Polym. Sci.* **1999**, *71*, 1797–1808.
- (6) Chazeau, L.; Cavaillé, J. Y.; Perez, J. *J. Polym. Sci., Part B: Polym. Phys.* **2000**, *38*, 383–392.
- (7) Dufresne, A.; Vignon, M. R. *Macromolecules* **1998**, *31*, 2693–2696.
- (8) Dufresne, A.; Cavaillé, J. Y.; Helbert, W. *Macromolecules* **1996**, *29*, 7624–7626.
- (9) Flandin, L.; Hiltner, A.; Baer, E. *Polymer* **2001**, *42*, 827–838.
- (10) Juvin, P.; Hasik, M.; Fraysse, J.; Planès, J.; Pron, A.; Kulszewicz-Bajer, I. *J. Appl. Polym. Sci.* **1999**, *74*, 471–479.
- (11) Olinga, T. E.; Fraysse, J.; Travers, J. P.; Dufresne, A.; Pron, A. *Macromolecules* **2000**, *33*, 2107–2113.
- (12) Djurado, D.; Nicolau, Y. F.; Rannou, P.; Luzny, W.; Samuelsen, E. J.; Terech, P.; Bee, M.; Sauvageol, J. L. *Synth. Met.* **1999**, *101*, 764–767.
- (13) Lesueur, D.; Colin, X.; Camino, G.; Albérola, N. D. *Polym. Bull.* **1997**, *39*, 755–760.
- (14) Ouali, N.; Cavaillé, J. Y.; Perez, J. *J. Plast. Rubber Compos. Process. Appl.* **1991**, *16*, 55–60.
- (15) Takayanagi, M.; Uemura, S.; Minami, S. *J. Polym. Sci., Part C* **1964**, *5*, 113–122.
- (16) Throughout the paper, no distinction is made between experimental mass fractions and theoretical volume fractions used by percolation theory: this is justified by the very close values of both polymer densities.
- (17) Rannou, P.; Nechtschein, M.; Travers, J. P.; Berner, D.; Wolter, A.; Djurado, D. *Synth. Met.* **1999**, *101*, 734–737.
- (18) Fedorko, P.; Fraysse, J.; Dufresne, A.; Planès, J.; Travers, J. P.; Olinga, T.; Kramer, C.; Rannou, P.; Pron, A. *Synth. Met.*, in press.
- (19) Planès, J.; Bord, S.; Fraysse, J. *Phys. Status Solidi B*, in press.
- (20) Pomfret, S. J.; Adams, P. N.; Comfort, N. P.; Monkman, A. P. *Polymer* **2000**, *41*, 2265–2269.
- (21) Basheer, R. A.; Hopkins, A. R.; Rasmussen, P. G. *Macromolecules* **1999**, *32*, 4706–4712.
- (22) Abell, L.; Pomfret, S. J.; Adams, P. N.; Monkman, A. P. *Synth. Met.* **1997**, *84*, 127–128.
- (23) Yang, C. Y.; Reghu, M.; Heeger, A. J.; Cao, Y. *Synth. Met.* **1996**, *79*, 27–32.
- (24) Ho, K. H.; Huang, S. K.; Hsieh, T. H. *Synth. Met.* **1999**, *107*, 65–73.

MA0104377